Department of Information Engineering and Computer Science

Bachelor's Degree in
Information and Communication Engineering

Final Dissertation

A study of the anisotropy of backscattering of the snowpack in multispectral data acquired by Sentinel-2 satellites

Supervisor
Lorenzo Bruzzone

Student
Lucrezia Tosato

Anno accademico 2019/2020

Acknowledgements

A big thank you to my family, especially my mother ***Elena*** *and my father* ***Claudio*** *who, with their tireless support, both moral and financial, have allowed me to get this far, contributing to my personal education.*
I would like to thank Professor L. Bruzzone, supervisor of this thesis, for having allowed me to carry out an internship in his laboratory and for having me supported by the engineer M. Santoni who, in addition to the help and great knowledge he gave me during all these months, has always been available and precise during the whole period of drafting and development of the project.
Without you I wouldn't have been so passionate about the subject without you!
A special thanks goes to my fiancé ***Luca****, my brother* ***Francesco*** *who in these three years have been the people who have made me grow the most and have always been close to me despite my difficult character, have had a decisive weight in achieving this result, the arrival and at the same time the starting point of my life.*
A big thank you to all my friends who have accompanied me on this path, in particular to my "Band": ***Giada****,* ***Sara****,* ***Irene****,* ***Giorgia*** *and* ***Barbara****, thank you for your support and for sharing the best "Campa" with me.*
A thought also for ***Gianmarco*** *e* ***Evelyn****, my best friends, advisors and listeners, always by my side and ready to comfort me.*
I dedicate this dissertation to all three of my grandparents, ***Emanuele****,* ***Alexandro****,* ***Ida****, who couldn't see my achievement but who always believed in me, and grandma* ***Imelda****, I hope I made you proud.*

Indice

Introduction

The proposed work aims to analyse the main parameters of the snowpack by referring to optical data acquired by ESA Sentinel-2 satellites: based on the relationship between backscattering and the angle of incidence of the wave coming from the sun, the aim is to explain the behaviour of the backscattering of the snow when the parameters of the latter vary.
The satellite acquisitions have been integrated with data coming from stations of detection close by. They have been chosen in such a way as to achieve the greatest possible similarity with the situations observed by satellite: importance has been given to the spatial proximity, trying to have a comparable snow situation..
All data of the Copernicus program are made available to users by the European Space Agency (ESA) free of charge.
Sentinel-2 acquisitions are made thanks to the passive sensor that samples on 13 spectral bands: four bands at 10 m, six bands at 20 me three bands at 60 m of spatial resolution, during the study we mainly used the normalized difference between B2 and B8 bands.
The scenarios to which this study looks at are many: Trentino-Alto Adige, the region in which is located the University of Trento, is an area where electricity is obtained almost entirely Many of these power plants depend on dams or watercourses whose flow is directly proportional to the melting of snow or ice.
Satellite data offers the possibility of verifying this information with greater capillarity and distribution than timely information.
Other areas that might be interested in the proposed analyses are the prevention of Avalanche risks, or the study of climate change in mountain or polar areas.
The situations identified by this study may provide the basis for going on to study the snowpack at an appropriate level of detail; if integrated with other available Sentinel-2 data (previous years, different areas, different sensors) a number of much greater case histories, advancing more precise indications compared to many other situations than in this study was not considered.
Think of the potential of a system that can to accurately indicate areas of high danger, day by day, and with very high accuracy.
The study focuses on the anisotropy of snow: its backscattering varies according to the conditions of the snow and depending on the angle at which it affects the sunlight (SLIA).
I want to propose a thesis that explains the behavior of backscattering distribution depending on snowpack and SLIA conditions.
In this way it is possible to outline the main characteristics of the blanket, such as hypothetical composition and humidity of the snow, corroborating the claims made with the snow data on the ground provided by Meteotrentino.
Some case histories have been proposed that support the previous hypothesis, as well as some comparisons with different cases coming out of the ordinary snowpack situation.

1 Background

1.1 Measurements of the Anisotropy of Reflectance of Ice and Snow

Up to now, the studies concerning the backscattering characteristics of the anisotropy of the snowpack have been mainly carried out using active sensors, typically SAR.
The use of these instruments allows the analysis of the territory at any time, in any weather condition and also allows to make studies at different depths of the snowpack.
The difficulty of understanding, the intrinsic noise of these data and the high geometric distortions present in mountain areas create a significant amount of missing data that complicates the analysis, for these reasons in recent years we are trying to develop methods for the analysis of the snowpack through passive sensors, which have a higher degree of understanding of the data than the active ones, in addition the snow shows unique characteristics in the visible, infrared and thermal spectrum.
In particular, several analyses were carried out by nivologists directly in the field using spectrometers and special chambers: a new method to determine the reflectance anisotropy of sea ice and snow at spatial scales from $1m^2$ a $80m^2$ using a circular multi-spectral infrared fish-eye camera (CE600) was made in 2018 [1].
CE600 allows to simultaneously measure radiance in all directions of a hemisphere at an angular 1° resolution.
The spectral characteristics of the reflectance and its dependence on the obtained lighting conditions from the camera are compared with those obtained with a hyperspectral field radiometer spectrum produced by Analytical Spectral Device, the evaluation of wavelength dependence has shown that models for snow, bare ice, and tinned ice surfaces are very similar whatever the spectral band considered.
This means that if the surface reflectance at a given wavelength increases/decreases in a given direction (for example, in the direction of specular reflection), the surface reflectance can be expected to increase/decrease at all wavelengths in this particular direction.
However, it has been observed that the rate of increase/decrease depends on the wavelength.
The concept has been further developed to define clusters formed by highly correlated pairs of wavelengths for snow and icy surfaces, a first cluster with the blue and NIR bands and a second cluster with the green and red bands is defined. Other studies[2] were carried out directly in laboratories after samples of different snow types were taken in situ at different depths of the snowpack, with the main focus on backscattering at near-zero angles using goniometers.
The studies have detected a perpetual peak at 0° of incidence (visible only through beam splitter), a stronger backscattering of fresh snow compared to frozen snow and a variable trend depending on the grain size.
When comparing samples at freezing temperatures, the shape of the curve appears more pronounced for those with larger grains, while smaller peaks occur for those with a grain size of 0.5 mm or less.
Samples with large grains have mostly lower reflectance, which underlines the relative increase towards

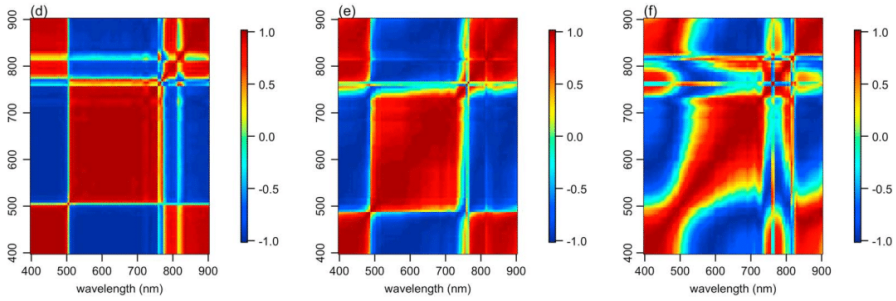

Figura 1.1: Correlation between the bands in c)Snow d)Ice e)Dirty ice)[1]

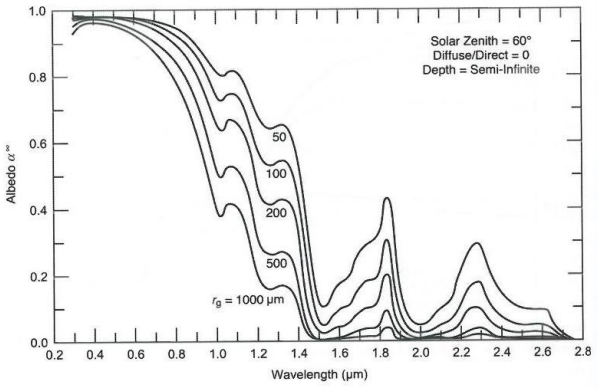

Figura 1.2: Spectral reflectance of the snow as the size of the grain radius changes[3]

0°.
In summary, in proportion, the peaks detected are more accentuated for large grains, which have less reflectance for the rest of the angles, while smaller grains are subject to larger values, which is why the peak is not so evident.
This is in agreement with the results of J.Dozier's 2004 study[3](Fig.1.2), for which samples with grain size less than 1 mm generally produced higher values.

In a third job[4] carried out on the anisotropy of the snowpack is reported starting from the observations made by Steffen[5], Perovich[6] e Grenfell[7] that the anisotropic reflectance for old snow is very high, similar values can be found in Arctic and Antarctic snow, both dry snow situations, values higher than those mentioned above were only detected in glaciers.
Also low solar elevations, which occur at high latitudes, they also increase the degree of anisotropy of the reflected radiance, either snow that ice are highly sensitive to solar elevation and the increase in the solar zenith angle increases overall anisotropy of reflection for all types of snow.

1.2 Estimation of Surface Snow Wetness using Sentinel-2 Multispectral data

In order to be able to discriminate the humidity of the snow, several researches have been carried out [8], a proposed approach is based on the triangle method which is used significantly for the assessment of soil moisture.
A triangular spatial feature is developed using near infrared (NIR) reflectance and normalized index (NDSI).
Based on the assumption that the NIR reflectance is linearly correlated with the liquid water content in the snow, a physical relationship is derived for snow estimation wet, the results of the snow moisture model were compared with the in situ measurements of the surfaces snowy and an error rate of 0.535 between estimates and measurements was observed.
The reflectance of the snow is reduced as the snow ages and crystallizes after constant melting and refreezing processes that result in an increase in snow grain size and snowpack compactness.

In the NIR spectrum, reflectance shows greater sensitivity to the size of snow grains, dry snow has high reflectance and wet snow has lower reflectance.(Fig1.3).
It is possible to observe (Fig1.4a) that dry snow has a higher NDSI level and vice versa for wet snow, in general, for NDSI snow surfaces exhibits values greater than 0.4.
However, depending on many Factors such as the angle of illumination and the level of contamination of the blanket the threshold can change, usually NDSI greater than 0.7 represents dry or fresh powder snow.

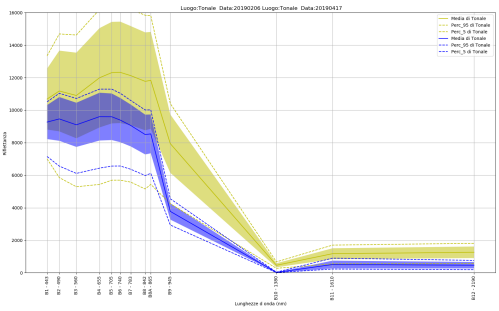

Figura 1.3: Confronto firma spettrale 06 Febbraio e 17 Aprile

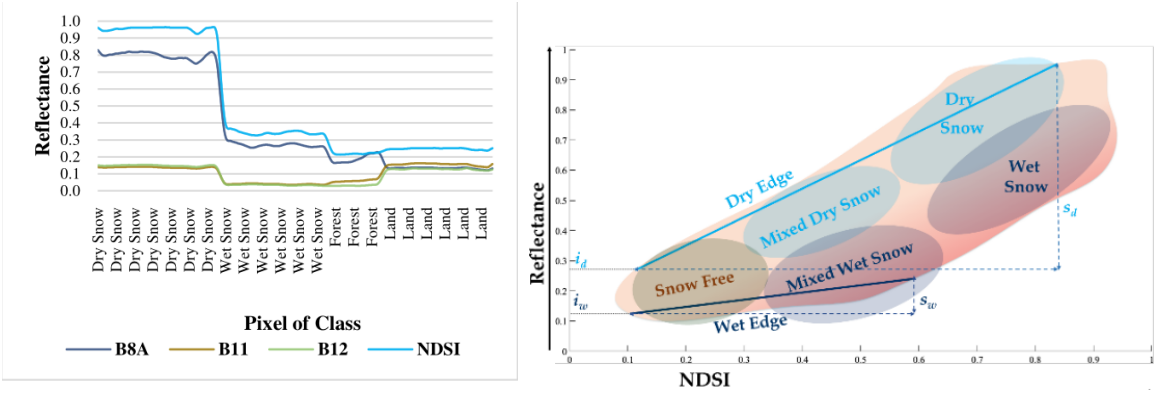

(a) Spectral response of different classes in the B8A bands and B11 and B12 compared to the NDSI[8]

(b) The general arrangement of dry and wet snow pixels in NIR-NDSI space[8]

Figura 1.4

1.3 Sizing of snow grains using backscattered sunlight

It is well known that the granulometry of the snow determines the level of light absorption by the snow and that this parameter is necessary to evaluate the thermal balance of the snow and also the time and extent of its melting. Starting from the notion that the near-infrared channel signals depend on the size of the grains[9], In fact, for this channel the optical granulometry is close to that measured in situ, but the reflectance of the derived snow is not accurate enough to allow a reversal of the granulometry with respect to reflectance.

For the mid-infrared channels, the calculated optical grain size is very different from the measured one, but a linear relationship between these different sizes was found for the April and December data, despite the very different solar radiation conditions.

The use of channel ratios instead of a single channel provides only a qualitative estimate of the grain size.

In 2011 a job was proposed[10] to validate a new snow grain size recovery algorithm.

The correlation coefficient between satellite and terrestrial measurements was in the range 0.6-0.7, these low values could be due to different size definitions in ground and satellite measurements.

The first issue they addressed was the definition of particle size.

The crystals in the snow have different shapes and do not resemble simple spherical particles such as those that occur, for example, in mists and water clouds. Therefore, various sizes of snow grains are measured and reported.

However, as far as remote sensing is concerned, the detailed structure of the snow grains is not accessible.

Only the actual optical size of the grains can be obtained, the notions of average volume V and average projection area S of the crystals can be used to define it.

These parameters exist for any grain and, in principle, can be measured.

The effective grain size (EGS) a_{ef} as the ratio of these parameters:

$$a_{ef} = \frac{V}{S} \cdot k \tag{1.1}$$

The parameter k = 0.75 is introduced so that the value of a_{ef} is equal to the particle radius for the case of monodisperse sets of spheres.
In the case of spherical polydispersions, a_{ef} has the simple meaning of the relationship between the second and third moment of size distribution.
As theoretical modeling demonstrates[11], the absorption cross-section C_{abs} of snow grains in the weak region The absorption of light is proportional to the volume of the grains, regardless of their shape.
Therefore, it follows that

$$C_{abs} = A \cdot \alpha \cdot V \tag{1.2}$$

where A is a constant that depends on the actual shape of a grain and also on the actual part of the refractive index.
However, the method presents several problems in wet snow cases, in the presence of pollution and in the detection of grains at greater depths.

1.4 Analysis, formation and variations of the snowpack

The crystals, complex and multiform elements, are characterized by continuous transformations[12] because of their often near melting point state.
After the snow crystals form in the atmosphere and take on a shape and direction of growth based on temperature and percentage of humidity(Fig. 1.5) present in the clouds, these undergo two phases of metamorphosis:

- Snow Metamorphosis in Atmosphere
- Snow Metamorphosis in Soil

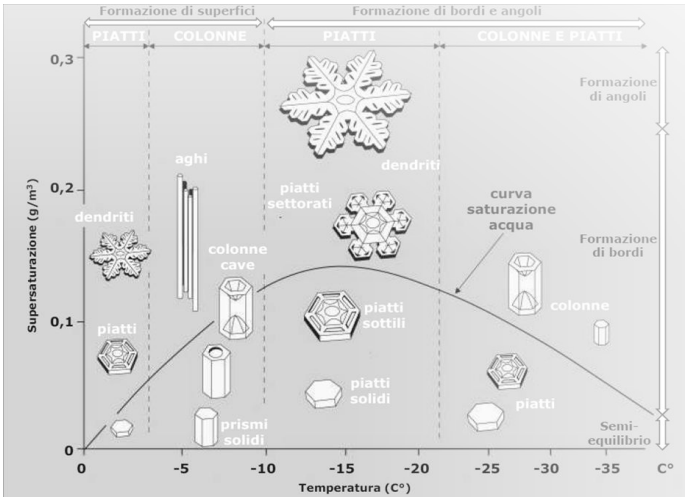

Figura 1.5: Formation of snow crystals as a function of excess steam density and temperature[12]

During the first metamorphosis the ice crystal is in its path from the cloud to the ground, hardly ever arrives unharmed at its destination and can undergo a series of metamorphisms that determine the change of shape or even a change of state from solid to liquid.
The metamorphism taken into consideration is destructive, influenced by isothermal energy or the mechanical effect of wind.
In both cases, from crystals of dendritic shaped fresh snow, you switch to rounded shapes.
The snow crystal once it reaches the ground, finding a new environment compared to the formation

one, is subject to a series of transformations in a number of ways and different times called metamorphisms on the ground.
Depending on the conditions environmental this set of processes lead to variations in the structure of the snow due to various factors such as: temperature, wind, geothermal heat flow, pressures, solar radiation (incident and reflected), radiation night with clear skies and fog.
From these factors it can be seen that the heat exchange (heat is both given up and acquired) between snow and the ground and the atmosphere, allows the evolution of the snowpack determining the distribution of temperatures inside it and consequently the metamorphisms.
The thermal exchange(Fig. 1.6) defines the gradient thermal inside the snowpack: change in temperature starting from snow on the ground, up to the surface, measured in degrees centimetre [°C/cm]. It is established in the snowpack and develops in the layers with three types of thermal gradient

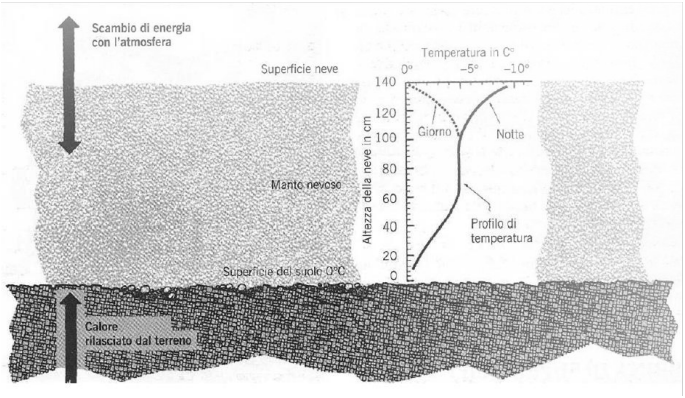

Figura 1.6: Illustration of temperature variations in the snowpack

corresponding to three types of metamorphism:

- **High gradient:** greater than 0.2°C/cm, allows constructive metamorphism with strong kinetic growth of crystals.
  These newly formed crystals constitute the frost of depth and tend to take the form of a goblet because of the subsequent deposit of thin ice flakes with flat stepped facets and to achieve dimensions even larger than 10mm.

- **Medium gradient:** between 0.05°C/cm and 0.2°C/cm, is characterized by destructive metamorphism slow or slight kinetic growth of crystals.
  The medium gradient metamorphism creates grains that have a low cohesion and consequently the snowpack becomes unstable.

- **Low gradient:** values below 0.05°C/cm involving destructive metamorphism.
  In this case the particles after about 24h begin to take on a progressive rounding form with small grains that gradually increase the their volume becoming rounded grains.
  Low-grade metamorphism or destructive metamorphism, it's as much as fast as the temperature of the snow is approaching at zero heat.
  At low temperatures, however, such transformation is slower.

An isothermal situation can also be established, with the absence of gradient thermal inside the snowpack and therefore with temperatures of 0°C almost constants in a vertical sense that gives rise to the fusion metamorphism and usually subsequent rigelo.
An important characteristic of the snowpack is the water content, this index measures the water content of the snow and is defined as the percentage of free water present in the volume, is a fundamental parameter for explaining, for example, the characteristics of the snow at the detachment, as it affects, together with the temperature, the metamorphism of the snow, determining the type of avalanche.
There are currently several methods of measuring water content: hot calorimetry (melting) and cold calorimetry (rigelo), dilution with dielectric measurements.
Liquid water becomes free only if the water content is exceeded. capillary. This value represents about

3% of the volume and depends on the snow texture, size and shape of the grains.
Capillary water is water that can be retained by surface forces against gravity.

d'umidità.

TERMINE	CONTENUTO IN ACQUA	NOTE
Asciutta	*0%*	La temperatura è solitamente *<0°C*, ma si può avere neve asciutta fino a *0°C*. I grani di neve hanno una scarsa tendenza ad unirsi.
Umida	*<3%*	*T=0°C*. L'acqua non è visibile nemmeno con ingrandimenti *10X*. Quando viene schiacciata leggermente la neve ha una netta tendenza a restare unita.
Bagnata	*3-8%*	*T=0°C*. L'acqua è riconoscibile con ingrandimento *10X* tramite il suo menisco tra i grani contigui; non è comunque possibile estrarre l'acqua schiacciando moderatamente la neve tra le mani.
Molto bagnata	*8-15%*	*T=0°C*. L'acqua si può estrarre premendo moderatamente la neve; vi è però ancora una certa quantità d'aria all'interno dei pori.
Fradicia	*>15%*	*T=0°C*. La neve è impregnata d'acqua e contiene una quantità d'aria relativamente limitata.

Tabella 1.1 Classificazione manto nevoso in funzione dell'umidità [3].

Figura 1.7: Illustration of temperature variations in the snowpack[12]

1.5 Data interaction between the passive sensor and the snowpack

The dawn of snow, as emerges from an article by Warren Wiscombe(1980)[13] is influenced by the characteristics of the snow itself:

- **Grain size or age:** These two characteristics are correlated as the ageing of the snow grain leads to its expansion.
  It has been observed that the metamorphosis of snow grains follows the same relationship as the grains grown by sintering in metal and ceramics:

$$D^2 - {D_0}^2 = \alpha t e^{-\frac{\beta}{T}} \tag{1.3}$$

  Where D is the grain diameter, t is the time, T is the temperature in degrees Kelvin and α e β are constant. Ageing and increasing size lead to a decrease in albedo, particularly in the bands beyond the visible. The explanation for this is that the larger the grains the more absorbent they are and the greater the scattering, i.e. they are less isotropic.

- **Liquid content:** As the water in the grains increases, the albedo decreases. The explanation of this event is due to the fact that water replaces the air between the grains of ice, the spectral reflectance of liquid water is very similar to ice for wavelengths under 5μm and the replacement of water instead of air increases the magnitude of the wheat also accelerates the growth rate of wheat.

- **Solar Zenit Angle:** Albedo increases with increasing zenith angle in all lengths but is more evident in the near-infrared lengths. The considerations regarding the zenith angle are not always reliable as many instruments do not show a true response to the cosine rule which leads them to overestimate the albedo at a certain angle. Moreover, if a thin layer of ice is present there will be a "glancing incidence" specular reflection phenomenon.

- **Cloud Cover:** The cloud cover influences the ghostly albedo of the snow converting direct radiation into diffuse radiation and thus changing the actual angle of the zenith. The explanation of this event is due to the fact that the direct conversion into diffuse radiation may or may not be opposite to the actual one and therefore increase or decrease the albedo, for high angles it decreases it for small angles it increases it.

- **Thickness of snow:** The thickness of the snow changes the albedo in an obvious way in the part visible of the spectrum. The smaller the grain radius is the faster the albedo will reach its asymptotic value, which is why it is a difficult phenomenon to study.

- **Snow Density:** The density of the snow was a function of the albedo, it is not yet sure whether this dependence derives from the fact that density is related to old age and grain size, it is not taken into account for the time being.

All these characteristics are decisive for determining what the sensor placed in the satellite will detect, and after processing the signal we will be able to view it from the ground.

1.6 Sentinel-2

Sentinel-2[14] is a mission developed by the European Space Agency (ESA) under the Copernicus programme to monitor areas of the planet and provide support in the management of natural disasters. It consists of two identical satellites, Sentinel-2A and Sentinel-2B launched on 23 June 2015 and 7 March 2017 respectively.
The Sentinel-2 satellites both mount a multispectral (MSI) device capable of acquiring images on 13 channels in the visible/infrared (VNIR) and shortwave infrared (SWIR) band, flying over the same point on the Earth's surface with the same viewing angle every 5 days, at higher latitudes the overflight of the surface is more frequent, but with different viewing angles.
Ground detail resolutions of 10, 20 and 60 meters depending on the spectrum band, the ground horizon is 290 km and all data are freely accessible.
To ensure high overflight frequency and continuous availability, two identical satellites (Sentinel-2A and Sentinel-2B) operate simultaneously on the same heliosynchronous orbit at 786 km height offset by 180 degrees.
Both satellites operate in two levels: 1C and 2A.
Level 1C represents the reflection at the top of the atmosphere, while level 2A is atmospheric corrected and shows the reflection at the bottom of the atmosphere.

1.7 Platforms and editors used

1.7.1 Google Earth Engine

The platform mainly used was Google Earth Engine [15], this combines a multi-petabyte data set of satellite images and geo-spatial data with analysis capabilities on a planetary scale, all made available for free to scientists, researchers and developers to detect changes, map trends and quantify changes on the Earth's surface.
The platform is used via Javascript commands.

1.7.2 Visual Studio Code

Visual Studio Code [16] is a free source code editor developed by Microsoft.
It includes support for debugging, built-in Git control, Syntax highlighting, IntelliSense, Snippet and code refactoring.
It can be used with various programming languages, in this case Python version 3.8.1.

2 Data

2.1 Sentinel-2

Each Sentinel-2 detection can contain multiple resolution cells and each pixel becomes a separate Earth Engine resource.
EE IDs for Sentinel-2 resources have the following format[17]:
COPERNICUS / S2 / 20151128T002653_20151128T102149_T56MNN.
The meaning is:

- **COPERNICUS**: Indicates the program you belong to
- **S2**: Indicates the satellite and the level being used
- **20151128T002653**: The first numerical part represents the date and time of detection
- **20151128T102149**: The second numerical part represents the date and time of product generation.
- **T56MNN**: The final string of 6 characters is a unique identifier that indicates the reference to the UTM grid of the pixel

2.2 Snow Camp

Data from the manual snow and weather stations of Passo Tonale Scuola Pat(1880 m, near the ski slopes) and Presena(2735 m) were taken into consideration.
Both in the winter period have daily update frequency of the station data snow.
The data we have considered are maximum and minimum temperature in the last 24 hours, instantaneous temperature, snowpack height and fresh snow height.

2.3 Penetrometric and Stratigraphic Profiles

The mod4 AINEVA(Fig. 2.1) of the Passo del Tonale(1880 m) and Presena(2735 m) localities were used, i.e. the most similar available locations (altitude and geographical proximity) to the area observed by satellite.

In this way it was possible to know the composition of the various layers in relation to the various types of snow crystals, the temperature of the environment and the various layers of snow.

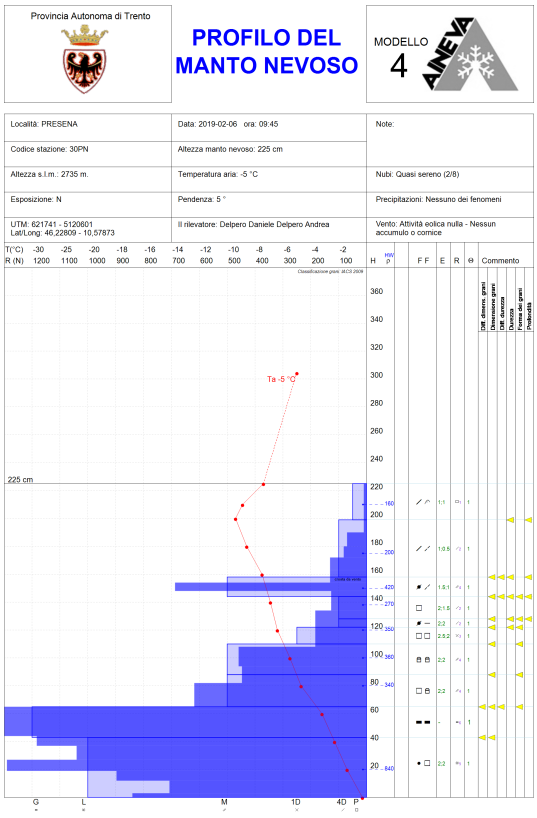

Figura 2.1: Graphic mod4 AINEVA(6 Febbraio 2019, Presena)

The data that we are most interested in are the humidity data. (Fig.2.2a) and the type of snow grains present (Fig.2.2b)[18].

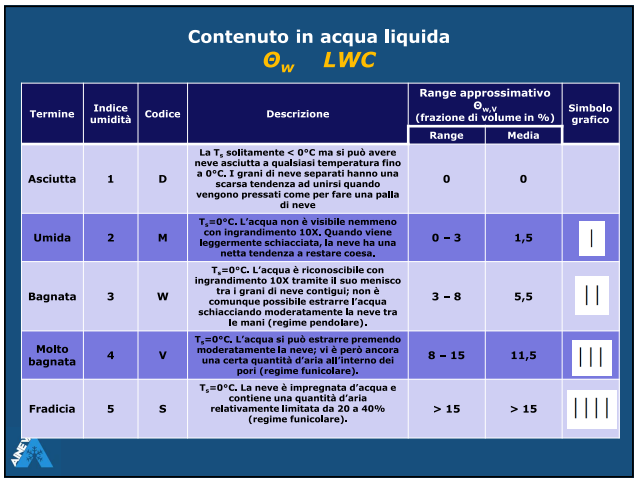

Contenuto in acqua liquida
Θ_w LWC

Termine	Indice umidità	Codice	Descrizione	Range approssimativo $\Theta_{w,V}$ (frazione di volume in %) Range	Media	Simbolo grafico
Asciutta	1	D	La T_s solitamente < 0°C ma si può avere neve asciutta a qualsiasi temperatura fino a 0°C. I grani di neve separati hanno una scarsa tendenza ad unirsi quando vengono pressati come per fare una palla di neve	0	0	
Umida	2	M	T_s=0°C. L'acqua non è visibile nemmeno con ingrandimento 10X. Quando viene leggermente schiacciata, la neve ha una netta tendenza a restare coesa.	0 – 3	1,5	|
Bagnata	3	W	T_s=0°C. L'acqua è riconoscibile con ingrandimento 10X tramite il suo menisco tra i grani di neve contigui; non è comunque possibile estrarre l'acqua schiacciando moderatamente la neve tra le mani (regime pendolare).	3 – 8	5,5	||
Molto bagnata	4	V	T_s=0°C. L'acqua si può estrarre premendo moderatamente la neve; vi è però ancora una certa quantità d'aria all'interno dei pori (regime funicolare).	8 – 15	11,5	|||
Fradicia	5	S	T_s=0°C. La neve è impregnata d'acqua e contiene una quantità d'aria relativamente limitata da 20 a 40% (regime funicolare).	> 15	> 15	||||

(a) Liquid water content

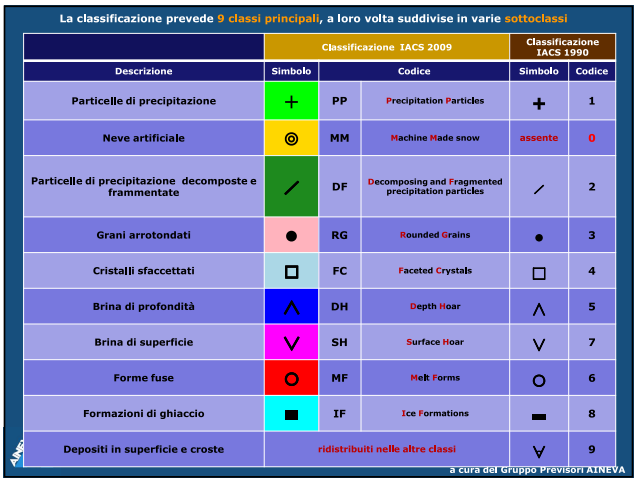

La classificazione prevede 9 classi principali, a loro volta suddivise in varie sottoclassi

Descrizione	Classificazione IACS 2009 Simbolo	Codice		Classificazione IACS 1990 Simbolo	Codice
Particelle di precipitazione	+	PP	Precipitation Particles	+	1
Neve artificiale	◎	MM	Machine Made snow	assente	0
Particelle di precipitazione decomposte e frammentate	⁄	DF	Decomposing and Fragmented precipitation particles	⁄	2
Grani arrotondati	●	RG	Rounded Grains	●	3
Cristalli sfaccettati	□	FC	Faceted Crystals	□	4
Brina di profondità	Λ	DH	Depth Hoar	Λ	5
Brina di superficie	V	SH	Surface Hoar	V	7
Forme fuse	○	MF	Melt Forms	○	6
Formazioni di ghiaccio	■	IF	Ice Formations	▬	8
Depositi in superficie e croste	ridistribuiti nelle altre classi			V	9

a cura del Gruppo Previsori AINEVA

(b) 9 Main classes of snow grains

Figura 2.2

2.4 Selected Dates

Using optical data it was essential to identify dates without cloud cover in order to carry out correct analysis, thanks to the large amount of data coming from the snow fields there were no problems in the choice even if we tried to favour dates where penetrometric and statigraphic profiles were also provided.
The dates were identified thanks to the use of EO BROWSER which allowed a visualization of all the data acquired by Sentinel-2 filtered by place and date.

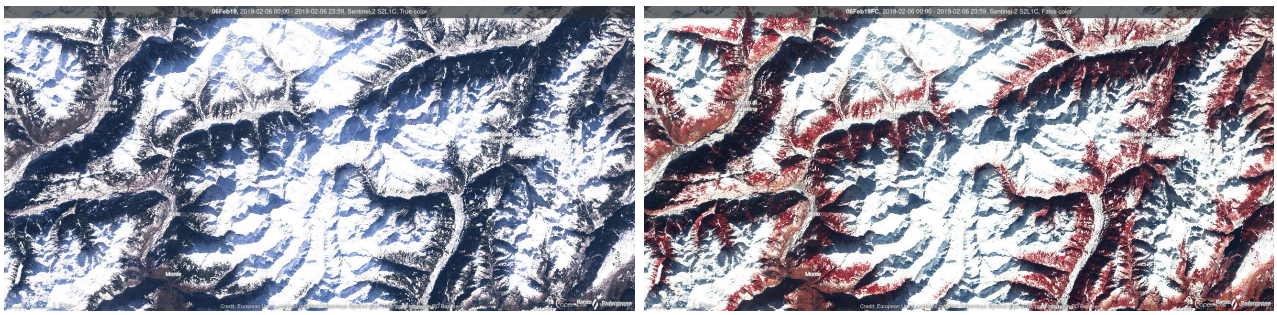

(a) RGB (b) False Color

Figura 2.3: February 6 2019

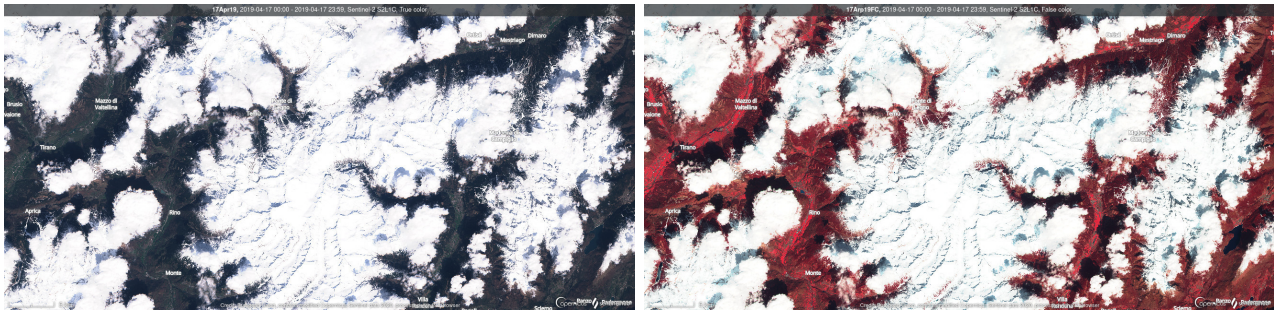

(a) RGB (b) False Color

Figura 2.4: April 17 2019

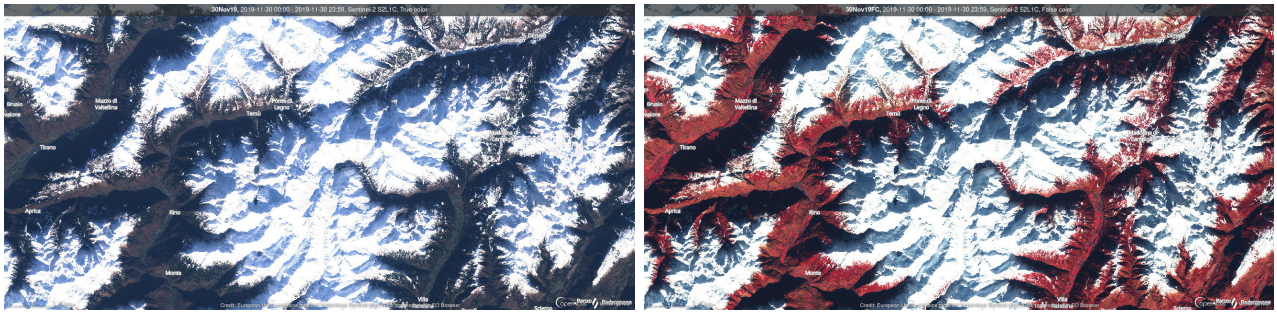

(a) RGB (b) False Color

Figura 2.5: November 30 2019

3 Method

3.1 Theoretical Scheme

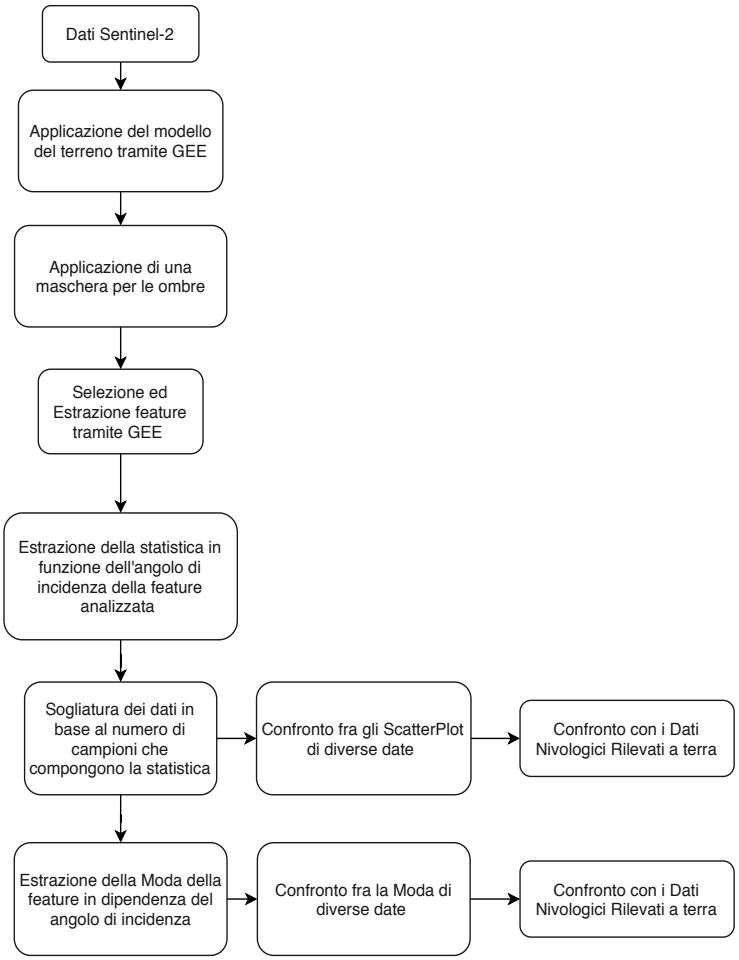

3.2 Application

During the development of the method a problem arose with the 2A level data because they were not properly corrected and had anomalies, because the snowpack was wrongly classified as a cloud and therefore corrected.
Because of this, artifacts are created in the images as visible in Figure **??**.
With the aim of developing a method for the analysis of backscattering of the snowpack under different conditions it was essential to identify dates to be studied.
As anticipated in the Chapter2.3 this was possible thanks to the information made available by Meteotrentino that allowed me to identify dates with particular snowpack conditions, by crossing these data with those coming from the EOBrowser it was possible to find the best dates on which to perform the analysis.
In order to produce an efficient analysis of the snowpack, I started from the spectral signature of the water in order to be able to suppose how this could be traced back to the variation of the snow.

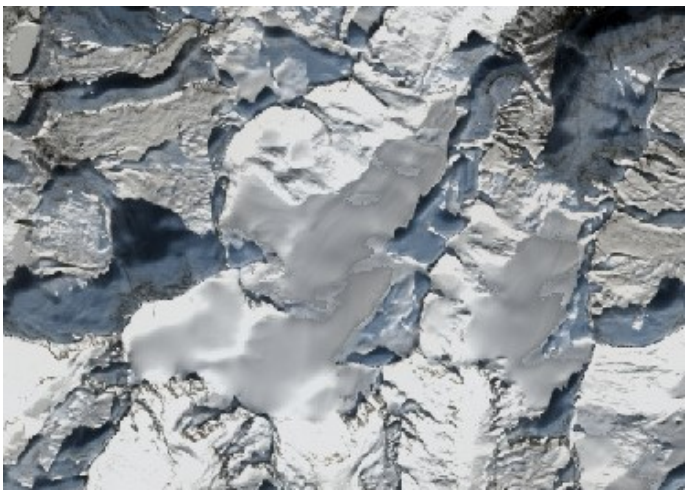

Figura 3.1: Adamello glacier level 2A

It is possible to notice(Fig.3.2) that the reflection peak of the water is found in the wavelength that

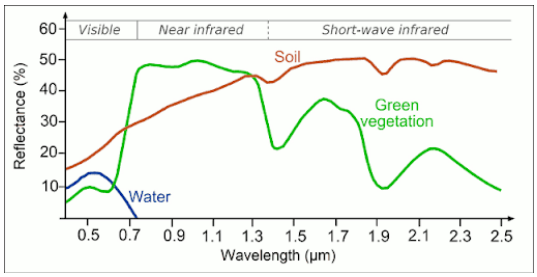

Figura 3.2: Spectral Water Signature

characterizes the blue color(0,450 μm) while in the near infrared the reflection is null.
For these reasons and with the support of articles by Warren Wiscombe(1980)[13], Dorothy K Hall(2004)[19] and Max Konig(2001)[20] I assumed that the normalized difference between the B2 and B8 bands could discriminate wet snow from dry snow.
The more the snowpack results to be in melting phase the higher will be the water content, consequently the index value will result positive thanks to a higher B2 band value and lower B8 band value, in presence of dry snow instead the water content will be reduced and the coefficient will result small or negative.

The study and application of this feature to Sentinel-2 data has been possible thanks to the use of

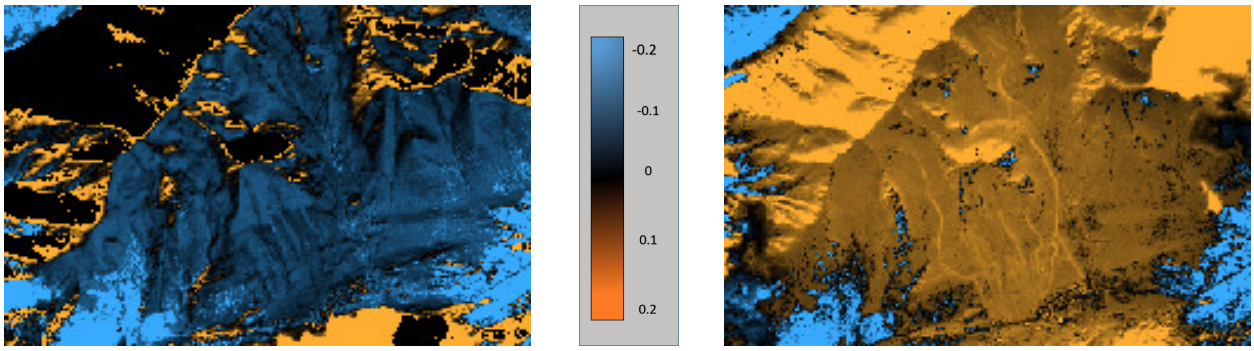

(a) February 6 2019 (b) Leg (c) April 17 2019

Figura 3.3: Example of index use

Google Earth Engine, as anticipated the level 2A data were not usable, so they were implemented directly on the platform of the masks that correct the data using the shadow model ("hillshade"),

based on the DEM terrain model, calculating it using the formula[25]:

$$IL = \cos(s_i) = \cos(Z)\cos(s) + \sin(Z)\sin(s)\cos(a - a') \tag{3.1}$$

And the angle of incidence of the local sun:

$$SLIA = Z - (s(a - \cos(a'))) \tag{3.2}$$

IL= lighting condition for each pixel at the time of image acquisition using a DEM
i_s= angle of incidence with respect to the normal surface
Z= solar angle of the zenith
s= slope of the ground calculated from DEM
a= solar azimuth
a$^{'}$ = aspect of the ground (azimuth) calculated from DEM
The DEM that has been used is "ALOS DSM: Global 30m". Another important fact that emerged from the documents is that fresh snow is more isotropic than old snow, so it radiates in every direction. This means that the reflectance of fresh snow follows the sun's incidence pattern less, while the reflectance of old snow follows it more.
Comparing the February and April images with those of the sun incidence model (Fig. **??**) one can see that the February image is closely related to it, while the April image has some slight differences, in fact the February snow was much older than the April image. I started from the feature normalized

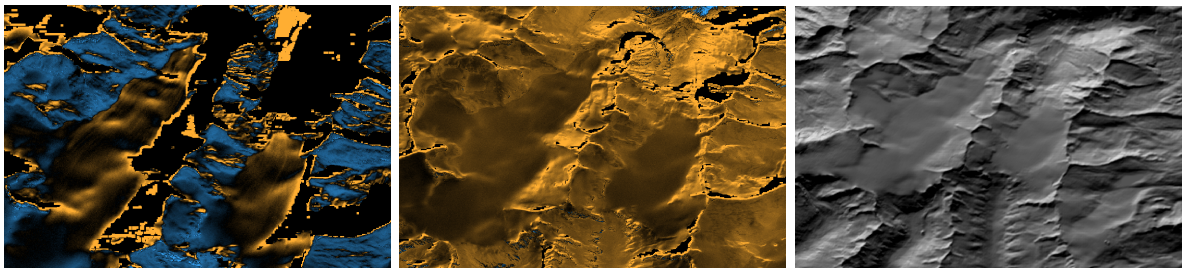

(a) February 6 2019 (b) April 17 2019 (c) Sun incidence model

Figura 3.4: Example of the different isotropic characteristics of snow in the Adamello Glacier

difference between the bands B2 B8 which was sensitive to the humidity of the and the anisotropy of the snow to carry on the analysis on the anisotropy, the areas chosen for the analysis had wide variations of angle of incidence and make a statistic of the values of the feature, how the feature varies as a function of the angle through a scatter plot.
The shaded areas create unbalanced feature values because the illumination source is no longer the sun but is the atmospheric scattering that illuminates the ground, therefore changing the spectral signature of the illumination source also changes the spectral signature of the object of our study.
For these reasons I went to exclude both with a mask and manually the shadow areas in order not to have wrong values.
The results of the scatter plots processed by GEE were not informative enough, a problem due to the maximum number of samples that the platform can extract, in fact the graphs could only contain 5000 samples.(Fig.3.5).
For this reason I exported the values in cvs format to the drive, from which they are then extracted and processed by another program.
In addition, the scatter plots, although characteristic, present for each angle of incidence a variable number of samples and then it is difficult to analyze the data being often misrepresented by the density of samples rather than their value.
For this reason, histograms were made to make the data clearer:

- As a first step we have defined intervals of incidence angle.

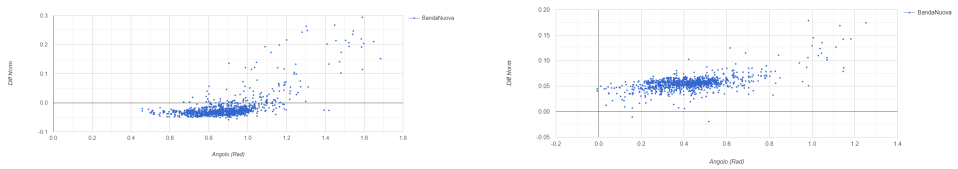

(a) 6 Febbraio 2019 (b) April 17 2019

Figura 3.5: Formati del diagramma di dispersione tramite Google Earth Engine

- In the same way a series of y-axis intervals have been defined (in this case the normalized difference B2,B8), creating a grid.
- With all samples belonging to a given column the histogram with respect to the intervals of the y-axis has been defined, the vector obtained will compose the respective column of the final matrix. In this way in each cell we obtained the number of samples of that given column that have value included in the interval of that row.
- Dividing all the values by the sum of the respective column we went from a number of occurrences to a value between 0 and 1.
- Finally, it is possible to impose a threshold related to the height of the sample position and a threshold related to the number of samples present in a column.

At this point the matrix describes the distribution of the value of the features under analysis as a function of the angle of incidence without being affected by the number of samples present.

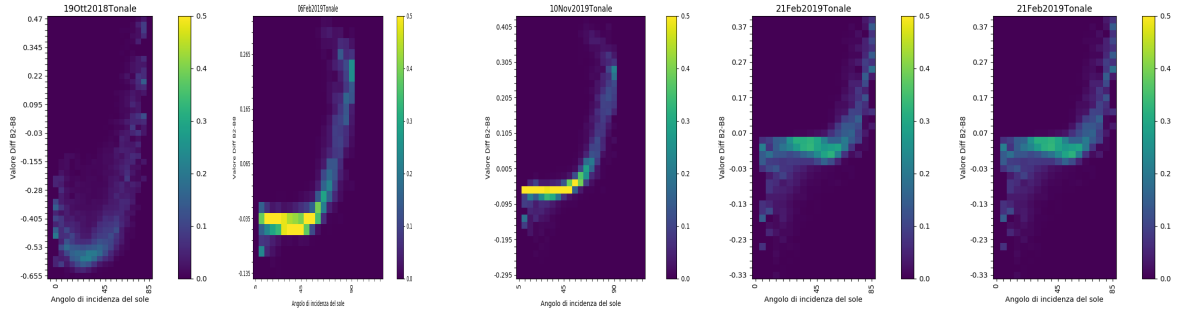

(a) Oct 19 2018 (b) Feb 6 2019 (c) Nov 10 2019 (d) Feb 21 2019 (e) Dic 28 2019

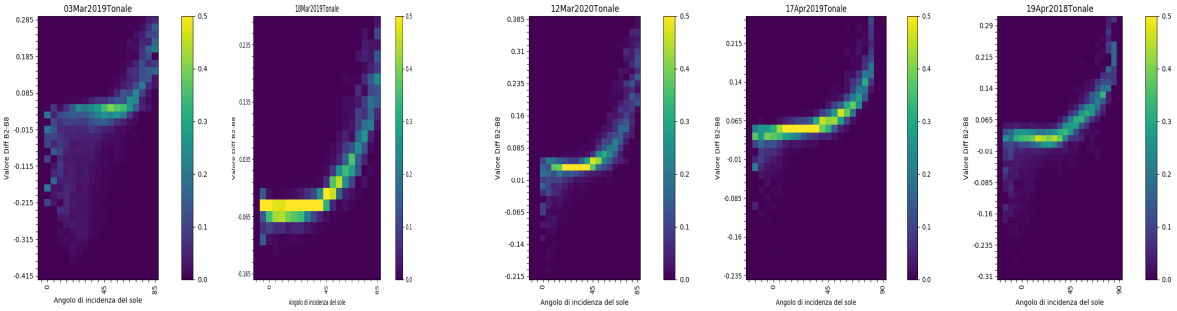

(f) Mar 3 2019 (g) Mar 18 2019 (h) Mar 12 2020 (i) Apr 17 2019 (j) Apr 19 2018

Figura 3.6: Histograms

In order to better visualize the trend of the curve and to be able to compare the results of different dates, the fashion of these functions has been implemented, making them for the greater value for each column of values.
To improve the visual quality of the graphs has been used the Savitzky-Golay function, a digital filter

that can be applied to a set of digital data points in order to smooth the data, that is, to increase the signal-to-noise ratio without significantly distorting the signal.

At this point it is possible to re-create the ScatterPlots after having set a threshold to all the data,

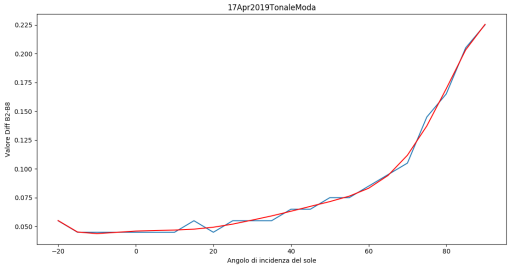

Figura 3.7: Savitzky-Golay

in order to eliminate the columns containing too few values and which may offset the results.

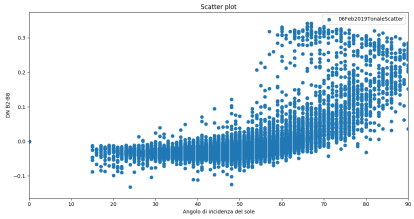

(a) February 6 2019

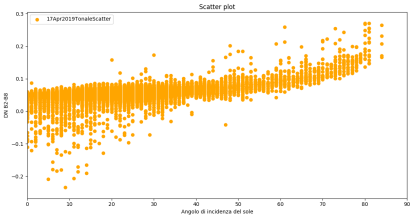

(b) Aprile 17 2019

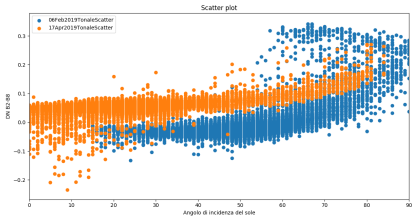

(c) Union of the two Scatter Plots

Figura 3.8: Scatter Plot

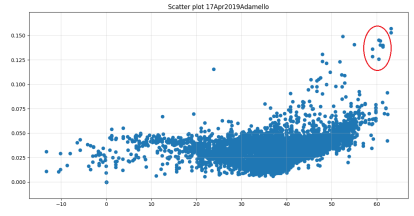

(a) Before

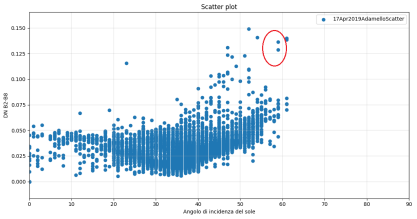

(b) After

Figura 3.9: Variation in ScatterPlots after data thresholding

4 Results

In relation to a thesis[21] already carried out concerning similar topic in SAR data, dates with similar conditions to the named study were chosen in order to possibly compare the results of the two studies.

Considered dates Tonale	Temp.	Snowfall	Grain Characteristics
Feb62019	Low	Present	Dry,T=-6°C,r=0.5
Nov102019	Low	Present	T=-2°C,
Dic282019	Modest	No	Dry - Damp ,T=-3C,r=1
Feb212019	Modest	No	Dry,T=-6°C,r=1
Mar32019	High	No	T=-2°C
Mar72019	Low	No	T=-2°C
Mar182019	Modest	Slight	Dry,T=-5°C,r=2-5
Apr192018	High	Present with rain	Wet,T=0°C,r=2-3
Apr172019	High	Present with rain	T=0°C
Mar122020	High	No	Wet,T=0°C,r=0.5

Considered dates Presena	Temp.	Snowfall	Grain Characteristics
Feb62019	Low	Present	Dry,T=-11°C,r=0.5
Nov102019	Low	Present	Dry,T=-8°C,r=1-1.5
Dic282019	Low	Slight	Dry,T=-10°C,r=1-0.5
Feb212019	Low	No	Dry,T=-8°C,r=1-1.5
Mar32019	Low	No	T=-9C
Mar72019	Low	Slight	Dry, T=-8°C, r=0.5-0.8
Ma18r2019	Low	Present	T=-8°C
Apr192018	High	Present	Damp, T=-1°C, r=0.8
Apr172019	Modest	Present	Dry,T=-1C,r=0.5
Mar122020	ND	ND	ND

4.1 Analysis 1: absence of snow vs presence of snow

The first proposed analysis aims at observing the trend of the basckscattering curve in conditions of absence of snow compared to dates when snow was present.
The acquisition was made on October 19 2018: the conditions should be ideal as there is low humidity and the ground has had the opportunity to lower its surface temperature.
It is evident that the feature values are far below the dates characterised by the presence of snow

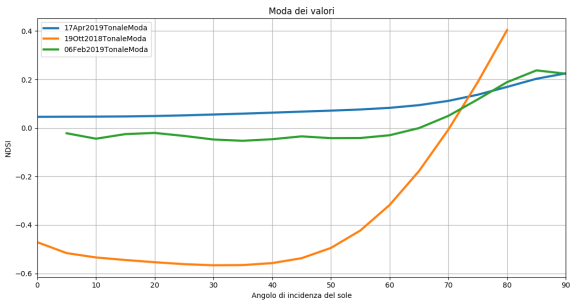

Figura 4.1: Mode of dates

because the difference of the B2 and B8 bands for the vegetation turns out to be a negative number,

in fact the NIR in the vegetation assumes very high values.
In addition, as the SLIA angles increase, the value increases considerably because the beam becomes more and more parallel to the ground showing in the backscattering the structure of the terrain.

4.2 Analysis 2: advanced melt state vs. fresh dry snow cover

Dates used to analyse backscattering during dry snow conditions(Fig. 4.2) were on 6 February 2019 and 10 November 2019(Fig. 4.2), the data we know about the snow cover of February 6 are: 92 cm of snow on Tonale, 210 cm of snow on Presena.
In addition, in the previous days there was a consistent snowfall (about 60 cm) and the temperature of the following days was rigid: therefore the snow did not have the chance to transform.
As confirmed by the penetrometric profile carried out at Passo del Tonale on the same day, we can affirm that the upper layer of the mantle is composed of fresh and dry snow.
In November the situation of the mantle was very similar even if the snowfalls were not as abundant as in the first case.

Dates used to analyse backscattering during wet snow conditions(Fig. 4.3) were 17 April 2019, 19

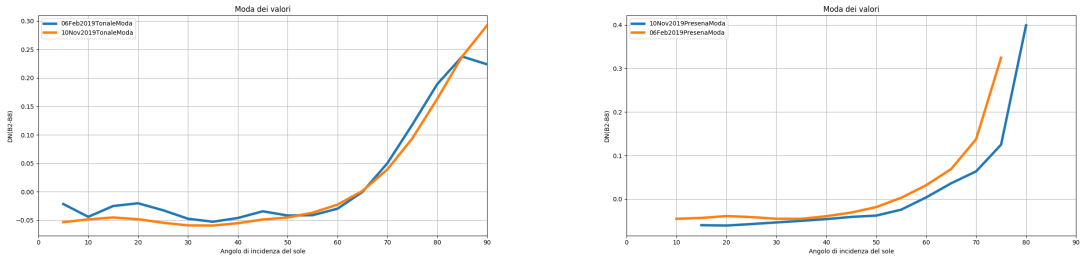

(a) Tonale (b) Presena

Figura 4.2: Mode of dates

April 2018 and 12 March 2020 the data we know about the snow cover of the first two days are that in both cases in Tonale there had been several snowfalls and rains in the previous days, in addition the temperatures were high.
It can be assumed that the snow would have been wet and the penetrometric data of 19 April 2018 confirm this hypothesis.
As for the third date, there had been neither rain nor snowfall in the previous days but the temperatures were high.
No dates with such distinctive characteristics have been found in Presena.

A comparison between a date with dry snow and a date with wet snow(Fig. 4.4) shows the differences

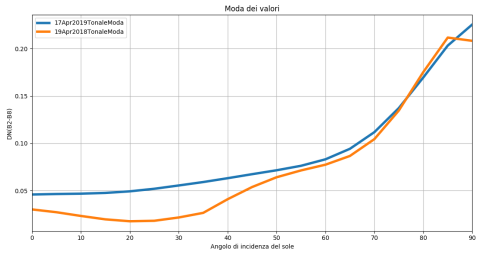

Figura 4.3: Modes of dates on Tonale

between the backscattering of the two types of turf.
It can be seen(Fig 4.4) that the two types of snow have different curve patterns, when the snow is wetter the curve increases more slowly, especially from 40 degrees onwards, whereas when the snow is dry it increases faster, especially above 60 degrees.

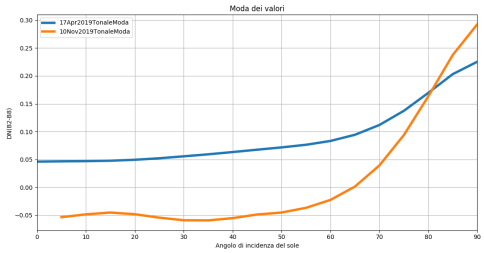

Figura 4.4: Mode of the most characteristic dates on the Tonale

4.3 Analysis 3: Dry snow on the surface and then wet

For the third analysis, the best dates to consider would have been 31 March to 6 April, as the time period is initially characterised by a week with very high temperatures (three days with maximum temperatures of 11°C), which led to the snow, which was already settled, increasing its melting and consequently its humidity.
Then, after 31 March, the temperatures dropped and between April 3 and 4 as much as 80 cm of fresh snow fell.

(a) March 31 2019 (b) April 6 2019

Figura 4.5: Hypothetical snowpack evolution for analysis 3[21]

Unfortunately, the days are characterized by a large amount of clouds that does not allow the analysis through multispectral sensors.
Instead, a date was chosen that is described by penetrometric bulletins as dry on the surface and wet afterwards: December 28, 2019.
Again, such special snow characteristics can only be found in the Tonale.
It can be seen(Fig. 4.6b) that the trend is similar to the case of dry snow, a predictable result due

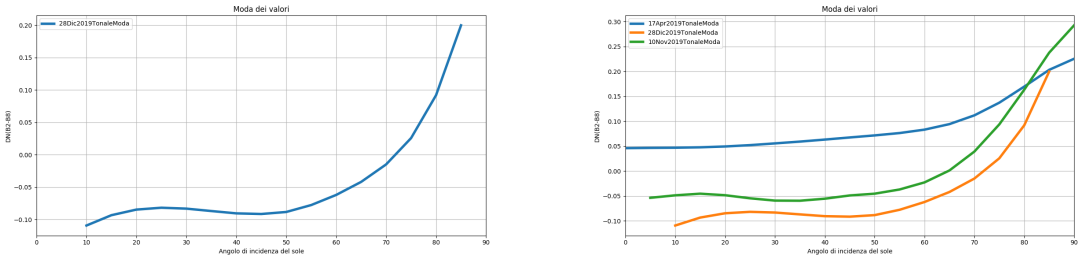

(a) Tonale (b) Tonale Comparison

Figura 4.6: Mode of dates

to the use of multispectral sensors that cannot penetrate more than a few cm into the surface.

4.4 Analysis 4: gradual settlement

It is very interesting to analyse the time interval between 17 February and 3 March: in this period there has been a gradual settling of the snow (in Tonale the decrease is 20 cm out of the initial 70 cm while in Presena it is 7 cm out of the initial 160 cm) with a present but relatively low melting: the Snow Water Equivalent (SWE) of the snow calculated in these weeks with the Tonale Pass data has

not decreased drastically.

The gradual settling does not present a characteristic curve, but it is possible to observe(Fig. 4.7)

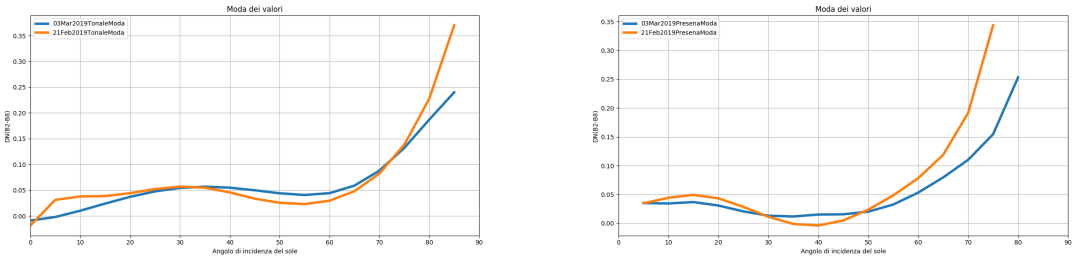

(a) Tonale (b) Presena

Figura 4.7: Mode of dates

how due to a slow melting of the snow and increasing temperatures the curve changed from being characteristic of dry snow to approaching that of wet snow.

4.5 Analysis 5: snowfall on settled snow

The fifth proposed analysis is based on three consecutive Sentinel-2 acquisitions.

In order to present a convincing hypothesis about the observed backscattering distribution, it is necessary to examine the temperature data from the week before the first acquisition.

The last week of February presented rather high temperatures, causing a transformation of the snow even at high altitudes: it can be seen in the date 3 March 2019, already taken into account in the Chapter 4.7, after which the temperatures decrease.

This may have favoured the formation of crust on the surface; the idea is that the backscattering trend has approached that of the dates with dry snow precisely because of the latter.

Then a snowfall occurred; the high temperatures of the following days, however, allowed a quick settlement of the 40 cm of fresh snow fallen on March 7.

The situation found by Sentinel-2 on March 13 could therefore be a compacted snow layer, resting on crust.

Due to the cloudiness the Tonale area did not bring useful information for the analysis, in particular March 8 and 18.

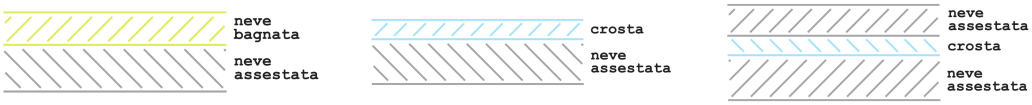

(a) March 1 2019 (b) March 7 2019 (c) March 13 2019

Figura 4.8: Hypothetical snowpack evolution for analysis 5[21]

The results obtained from the backscattering fashion (Fig. 4.8) seem to confirm the assumptions made, as the curve moves from an initial wet snow trend to a dry snow trend and then on March 13 to an intermediate situation.

A comparison of the three dates(Fig.4.9).

4.6 Analysis 6: Comparison with snowpack on glacier

This analysis was carried out in order to understand the differences in snow backscattering behaviour on the glacier compared to the situation considered so far. This analysis was done in order to understand the differences in the backscattering behaviour of snow on the glacier compared to the situation considered so far, also in view of future developments. It is possible to note (Fig. 4.11a) that in April the angles of solar incidence stop at 60, this fact is also present in April of the previous year (Fig.

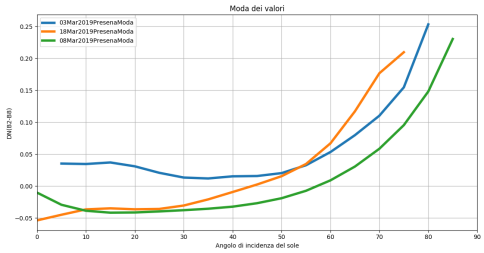

Figura 4.9: Mode of dates on Presena

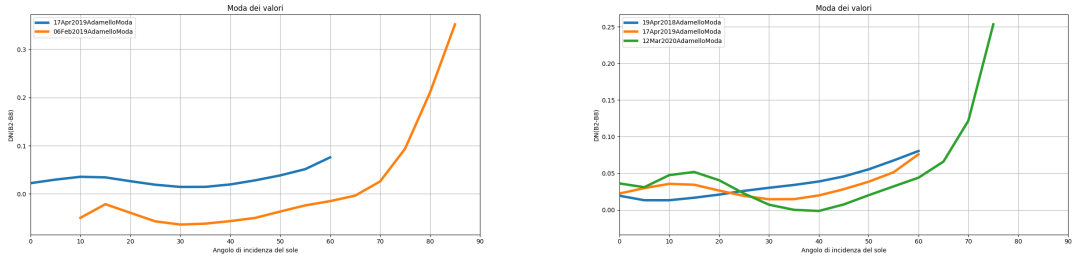

(a) Adamello on the most characteristic dates

(b) Adamello in all hot dates

Figura 4.10: Mode of dates

4.11b) probably because in April the sun is higher in the sky than in winter and therefore the range of present values of the SLIA is reduced depending both on the position of the sun and on the slope and exposure of the terrain.
The characteristics of the backscattering of the mantle seem to follow the trend described for Tonale under the same conditions, although unfortunately there are no penetrometric data for the area, so the hypotheses cannot be compared with concrete data.

4.7 Analysis 7: Comparison of neighbouring areas with different uses

The last analysis was made to understand what the differences in snow backscattering behaviour might be in two neighbouring areas of Tonale, one of them used for ski slopes and the other one free.

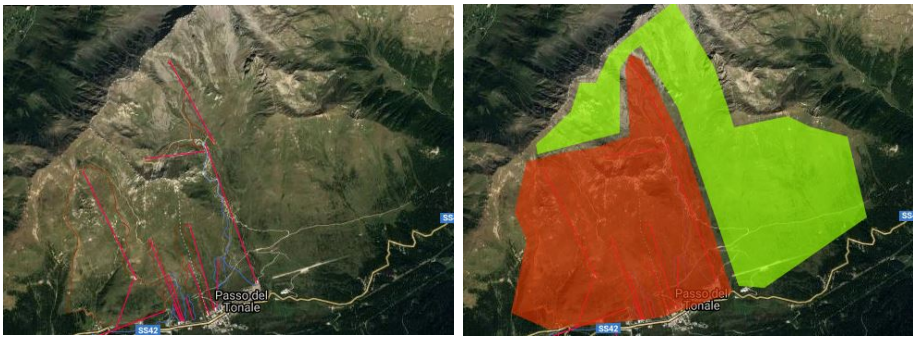

(a) Tonale

(b) Division of zones

Figura 4.11: Areas used for analysis

It is possible to verify (Fig. 4.12) how the surface changes in situations of use and non-use.
On the date of April 17, 2019 the ski season was in its closing phase, moreover the rains present in the previous days lead me to deduce that the slope had not been used.for this reason the variations between the two zones in the dates of April are minimal, while in February it is possible to notice more evident differences.

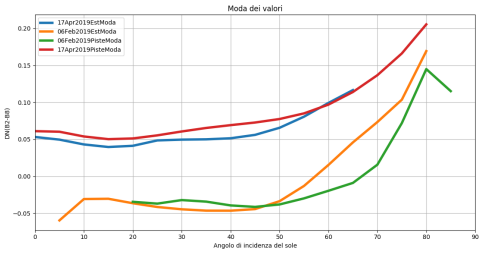

Figura 4.12: Comparison of the fashion of the most characteristic dates in the two zones

Potentially a similar pattern can be seen in the same areas, unfortunately these similarities being so small could have been created by the Savitzky-Golay function, surely this type of study would have the potential to be the subject of more in-depth analysis.

4.8 NDSI

Considering the NDSI trend as the angle of incidence varies on the main dates considered to be the most characteristic (Fig. 4.13), it can be seen that both in Presena and Tonale the values are always greater than 0.7, which means that the terrain is considered to be snow.[8].

It is possible to verify that on dates with wetter snow on the surface the NDSI values are greater

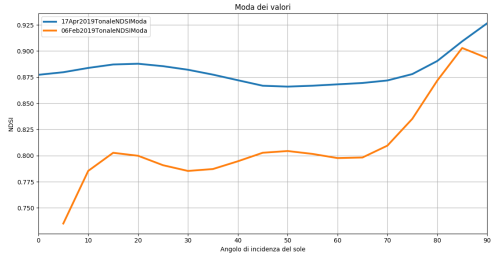

(a) Tonale

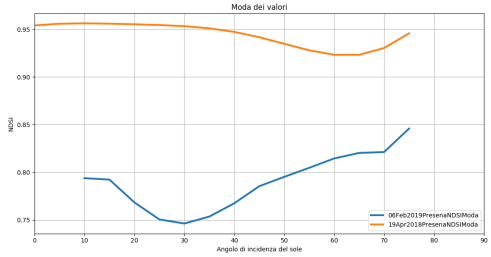

(b) Presena

Figura 4.13: Comparison of the NDSI fashion of the most characteristic dates

than on dates with dry snow, comparing this result with Figure1.2 it can be assumed that the wet grains are larger than the dry grains, a hypothesis in agreement with Warren Wiscombe's thesis[13].

5 Conclusions

In the presented thesis a method of analysis for Sentinel-2 optical data has been developed, with the aim of analysing the state of the snow. In particular, it is based on the analysis of the distribution of the normalised difference between the B2 (blue) and B8 (NIR) bands as a function of the angle of incidence; this normalised distribution has been represented by means of its mode.
The latter shows that the main variations in the values shown by the normalized difference in question depend both on the state of humidity of the snow and on the grain size, which can vary over time due to metamorphosis of the grains on the ground.
It can therefore be concluded that the normalised difference best represents the ageing state of the snow, which depends on all the transformations of the snowpack both in terms of moisture content and grain size.
The use of inter-channel ratios instead of a single channel provides a qualitative estimate of both grain size and snow moisture.
By using two bands subject to mathematical calculations it is not possible to refer to the literature on the subject, it is necessary to start from the literature and reason about the results obtained.
In our case (Fig. 5.1), for example, wet snow is always found to have greater values than dry snow, a result that would seem to contradict the theories proposed in the past.
However, if we go to reflect on the values of the bands used considering large wet snow, therefore large, and dry snow, therefore small, we can realize that the results, as verifiable in Figure1.2, depend on the increase of the reflectance in relation to the size of the grains and are consistent with the principles proposed.
Furthermore, as proposed by Wiscombe himself[13], below 50 degrees the snow albedo is independent of the solar incidence angle, which fits our results because with both types of snow up to 40 or 50 degrees there were no important variations in the albedo of the normalized difference.
It was found in the analysis (Fig. 5.1) that dry or fresh snow has lower values for most of the angles

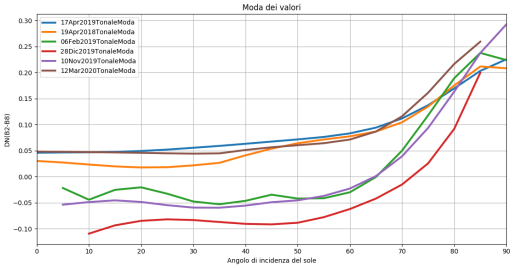

Figura 5.1: Comparison of the mode of the normalised difference of dates

of incidence of the sun, but for higher angles it grows much faster, a peculiarity that could be related to the structure of the snowpack that in dry snow conditions is complex and therefore there may be greater variations between the trends of the bands than in wet snow.
This theory is supported by Steffens[5], Petrovich[6] e Grenfell[7] which suggested that for higher SLIA angles there would be an increase in backscattering anisotropy.
The anisotropy of the backscattering present at high angles of incidence can be caused by the fact that the NIR reflectance decreases faster as the SLIA increases than in the visible bands, especially in dry snow which has, as mentioned above, a more intricate crystal structure.
In wet snow conditions the increase at higher angles is more attenuated, due to the fact that the snowpack is more compact and uniform and therefore the variation in the backscattering of the individual wavelengths should not change substantially.

The NDSI (Fig. refconfrontofinale2) also shows variations in the analysed dates, but these are smaller and less clear than those observed with the presented features.

In the future, it would be interesting to integrate this study with machine-learning algorithms that

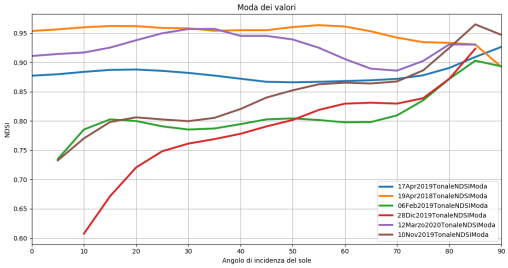

Figura 5.2: Comparison of the NDSI mode of dates

can automatically follow the proposed method and independently understand the main characteristics of the snowpack.

Such a tool would have enormous potential in the fields of avalanche prevention, snow conditions with a view to water supply to power stations, climate change studies or even analyses of snowpack pollution.

The study could be extended by applying methods for detecting the exact size of the snow grains, or by formulating more advanced analyses on hypothetically very interesting cases, such as the comparison between areas used as ski slopes and free neighbouring areas.

Furthermore, the bands used for the normalised difference are bands that are present in all satellites that mount passive sensors on board, so it could be widely used without requiring significant economic implications.

Bibliografia

[1] C. Goyens, S. Marty, E. Leymarie, D. Antoine, M. Babin, S. Bélanger. 2018.
High Angular Resolution Measurements of the Anisotropy of Reflectance of Sea Ice and Snow

[2] S. Kaasalainen, M. Kaasalainen, J. Suomalainen, J.I. Peltoneiemi, J. Naranen. 2006.
Optical properties of snow in backscatter

[3] J. Dozier, T.H. Painter 2004.
Multispectral and Hyperspectral remote sensing of alpine snow properties

[4] Z. Jin, J.J. Simpson. 2000.
Bidirectional anisotropic reflectance of snow and sea ice in AVHRR channel 1 and channel 2 spectral regions. II. Correction applied to imagery of snow on sea ice

[5] K. Steffen. 1987.
Bidirectional reflectance of snow at 500-600 nm

[6] D.K. Perovich. 1994.
Light reflection from sea ice during the onset of melt

[7] T.C. Grenfell, G.S. Warren, C. Peter. 1994.
Reflection of solar radiation by the Antarctic snow surface at ultraviolet, visible, and near-infrared wavelengths

[8] D. Varade, O. Dikshit. 2018.
Estimation of Surface Snow Wetness Using Sentinel-2 Multispectral Data

[9] M. Fily, B. Bourdelles, J.P. Dedieu, C. Sergent. 1997.
Comparison of in situ and Landsat Thematic Mapper derived snow grain characteristics in the alps

[10] A. Kokhanovsky, V.V. Rozanov, T. Aoki, D. Odermatt, C. Brockmann, O. Kruger, M. Bouvet, M. Drusch, M. Hori. 2011.
Sizing snow grains using backscattered solar light

[11] A. Kokhanovsky, E.P. Zege. 2004.
Scattering optics of snow

[12] A. Ferrari. 2015.
Le Proprietà Fisiche Del Manto Nevoso: Rilievo ed Elaborazionedi Dati Penetrometrici

[13] W.J. Wiscombe, S.G. Warren. 1980.
A Model for the Spectral Albedo of Snow.

[14] ESA
Sentinel-2

[15] Google Earth Engine
A planetary-scale platform for Earth science data & analysis

[16] Visual Studio Code
Code editing. Redefined.

[17] Google Earth Engine
Sentinel-2 MSI: MultiSpectral Instrument, Level-1C

[18] Scuola Intersezionale di Escursionismo Veronese. 2014.
Sistema di Classificazione del manto nevoso

[19] D.K. Hall, R.E. Kelly, J.L. Foster, A.T. Chang. 2004.
Estimation of Snow Extent and Snow Properties

[20] M. Konig, J.G. Winther, E. Isaksson. 2001.
Measuring Snow and Glacier Ice Properties from Satellite

[21] D. Mattedi. 2019.
Studio dell'anisotropia del backscattering del manto nevoso in dati sar acquisiti dai satelliti Sentinel-1

[22] N.Besic, G. Vasile, J. Chanussot, S. Stankovic, D. Boldo, G. D'Urso. 2013.
Wet snow backscattering sensitivity on density change for SWE estimation

[23] H. Rahman, D.A. Quadir, A.Z.M. Zahedul, S. Dutta. 1999.
Viewing Angle Effect on the Remote Sensing Monitoring of Wheat and Rice Crops

[24] Z. Li, H.K. Zhang, D.P. Roy. 2018.
Investigation of Sentinel-2 Bidirectional Reflectance Hot-Spot Sensing Conditions

[25] Open GeoBlog. 2018.
Topographic correction in GEE